ELSEVIER

Polymer Vol. 37 No. 6, pp. 969–974, 1996

0032-3861/96/$15.00+0.00

The relation between spinnability of thermotropic liquid-crystalline polymers and their submicrometre reinforcing function in polymer blends

Jiasong He* and Hongzhi Zhang
State Key Laboratory of Engineering Plastics, Institute of Chemistry, Academia Sinica, Beijing 100080, China
(Received 23 November 1994; revised 5 April 1995)

Six thermotropic liquid-crystalline polymers (TLCPs) were spun on a CSI 194 Mini-Max extruder in their optimized spinning-temperature ranges. Based on the diameter and the diameter distribution of the resultant fibres, these TLCPs were classified into two groups with good and poor spinnability, respectively. The viscosity ratio of TLCP to matrix resin, η_d/η_m, in the optimized spinning-temperature range was used as a parameter for controlling TLCP fibrillation in the resin matrix. For a TLCP having good spinnability, its morphology in different resins was observed and correlated with the viscosity ratio in the range of 10^{-2} to 10. With decreasing η_d/η_m from 16 to 0.05, the dispersed TLCP phase changes from spheres through ellipsoids and short rods to fibrils. Under the same condition, i.e. in the η_d/η_m range of 0.01 to 0.1, TLCPs with good spinnability generate fibrils in injection-moulded samples, while poor spinnability ellipsoids and rods only are generated. The results of image analysis show that two TLCPs with good spinnability generate fibrils of smaller diameters, narrower diameter distributions and larger intrinsic aspect ratios. It is shown that there is a correlation between the TLCP spinnability in air and TLCP fibrillation in the resin melt. This could be taken as a prerequisite for the achievement of submicrometre reinforcing with LCP fibrils.

(Keywords: polymer; liquid-crystalline polymer; spinnability)

INTRODUCTION

Thermoplastics can be reinforced by macroscopic fibres such as carbon fibre, glass fibre and aramid fibre (Kevlar). The macroscopic reinforcement increases the modulus and strength of composites. Thus in order to obtain a high-modulus and high-strength polymer composite, a higher percentage of fibre content (up to 30%, 45% and even 60%) is needed. The high percentage of filling will worsen the melt processability of matrix resins, wear processing machines and use more energy.

It is well known that, as the diameter of reinforcements decreases, their reinforcing effect will be more significant. Macroscopic fibres have diameters as large as several micrometres. Rigid-rod-like molecules of poly(*p*-phenylene terephthalamide) (PPTA) and the polybenzimidazoles (PBZs) can form microfibrils of 10–30 nm diameter[1]. However, the difficulties associated with processing these materials have thus far restricted the technology to the laboratory. Another approach to using rigid-rod or semi-rigid polymers as a reinforcing phase is to blend thermotropic liquid-crystalline polymers (TLCPs) with flexible thermoplastic polymers. The advantage of blending a TLCP with a thermoplastic polymer is that the TLCP can function as a processing aid and a reinforcing phase at the same time. For this reason, polyblends containing TLCP have become one of the hottest research topics in recent years[2–5]. A so-called *in situ* composite is fabricated by commonly used techniques such as extrusion and injection moulding, in which reinforcing TLCP fibrils are formed in the matrix by the shear or elongational flow of the blend melt.

Submicrometre reinforcing by means of TLCP fibrils has been achieved for thermoplastics. One of the crucial aspects for the reinforcing is the formation of TLCP fibrils having diameters of 10^{-1} μm and large enough intrinsic aspect ratios. The fibrillation of TLCP in thermoplastic melts is influenced by several parameters, including the thermal characteristics of the component polymers and their compatibility, processing parameters such as viscosity ratio, melt temperature, flow mode and shear rate[2–13].

Investigations on the morphology in Newtonian fluids and viscoelastic fluids have been conducted[14–20]. The deformation and break-up of the dispersed phase were correlated with the viscosity of the two components and the interfacial tension of the melt. However, for polyblends containing a TLCP the deformation and break-up of the dispersed TLCP droplets are more complicated. Up to now, though nearly all the isotropic polymers have been blended with TLCPs and the morphology has been investigated, the results are sometimes contradictory[13]. The parameters influencing the morphology of blends have been noted by most

*To whom correspondence should be addressed

Table 1 The average diameter of TLCP fibres obtained at their optimized spinning temperatures

Sample	Melt-temperature range (°C)	Optimized spinning temperature (°C)	Average diameter (μm)
TLCP1	280–350	280–350	56
TLCP2	250–330	300	42
TLCP3	275–320	300	43
TLCP4	250–380	310	128
TLCP5	295–340	330	134
TLCP6	190–240	220	133

researchers. However, the spinnability, one of the characteristics of TLCP itself, has not been noted fully[11]. The melt spinning of TLCP in air and the fibrillation in molten resin are correlated. The spinnability is affected by structural parameters such as bonding energy, spatial conformation, chain rigidity, molecular weight and molecular-weight distribution, as well as spinning parameters. In the present study, the spinnability of a TLCP is defined as the ability of the TLCP to be spun into a continuous fibre with the smallest average diameter under its optimized spinning conditions such as melt temperature and spinning speed. The melt spinning of TLCPs, the characterization of TLCP spinnability and the correlation between the spinnability and the fibrillation in matrix melt have been investigated.

EXPERIMENTAL

Materials

All of the thermotropic liquid-crystalline polymers used in this work are main-chain LCPs and are referred to as TLCP1–6, respectively. TLCP1 is an aromatic copolyester, Rhodester (Rhone-Poulenc, France). TLCP2 is *p*-hydroxybenzoic acid/poly(ethylene terephthalate) (PHB/PET) 80/20 (by mole) copolyester synthesized in laboratory scale. Its intrinsic viscosity (*IV*) is 0.84 dl g^{-1}, measured in phenol and 1,1,2,2-tetrachloroethane (1:1 by weight) at 25°C. TLCP3 has the same composition as TLCP2, with an *IV* of 0.67 dl g^{-1}. TLCP4 is a wholly aromatic copolyester synthesized in laboratory scale[21]. TLCP5 is PHB/PET 80/20 copolyester modified by naphthalene, produced by Chenguang Research Institute of Chemical Industry, China. TLCP6 is ethyl cellulose (EC), obtained from Shanghai First Preparation Factory, exhibiting its fluidity and some birefringent structure in the quiescent state above 207°C. It is taken as a thermotropic LCP[22]. Their melt-temperature ranges are shown in *Table 1*.

The five polymers used as the matrix are as follows: low-density polyethylene (LDPE, $M_w = 500\,000$, BASF); poly(ether sulfone) (PES, $IV = 0.38$ dl g^{-1} in *N,N*-dimethylformamide at 25°C, Jilin University, China); polystyrene (PS, B1, Lanzhou Chemical Industry Co., China); and two polycarbonates (Lexan-4490, $M_w = 27\,000$–$28\,000$, General Electric, denoted as PC-GE; and T1260, $M_w = 26\,000 \pm 1000$, Shanghai Zhonglian Chemical Factory, China, denoted as PC).

Spinning

TLCPs in the form of pellet or powder were melt spun with a CS-194 Mini-Max extruder equipped with a take-up roller of ca. 30 mm diameter. In the temperature range from their melting points to higher temperatures acceptable for spinning, a series of temperatures with a step of 5°C were used for spinning. At each temperature the rotation speed of the take-up roller was adjusted to as high as possible for spinning a continuous fibre. The temperature range in which the spun fibre had the smallest average diameter was taken as the optimized spinning temperature range for a certain TLCP. If a TLCP was spun at a temperature outside of its optimized spinning-temperature range, a continuous fibre with a larger average diameter or broken segments with smaller average diameter would be obtained. The results are shown in *Table 1*. In this paper, the optimized spinning temperature of each TLCP is called its characteristic temperature (T_c).

Before melt spinning all the TLCPs were dried for 8 h under vacuum at 100°C.

Blending and injection moulding

The melt blending of TLCP and the matrix thermoplastics was conducted on a CS-194 Mini-Max extruder in the composition ratio of 10 to 90 (by weight) at the T_c of the component TLCP.

Dumbbell samples of blends were injection moulded at the T_c of the component TLCP on a CS-183 Mini-Max injection-moulding instrument.

Wide-angle X-ray diffraction

The degree of orientation of TLCP fibres, spun under the optimized conditions, was characterized by wide-angle X-ray diffraction. Diffraction patterns were obtained at room temperature with an X-ray generator (JF-1, Dandong Instrument Factory, China), having Ni-filtered Cu K_α radiation and a flat-plate camera. The exposure time was 2 h at 40 kV and 25 mA.

Rheological measurement

The melt viscosity of TLCPs and their matched matrix polymers was measured with a Goettfert Rheograph 2001 capillary rheometer at the T_c values of TLCPs. A capillary die with an L/D ratio of 30 and a diameter of 1 mm was used.

Morphology characterization

The microstructure of all the samples was observed with the help of a scanning electron microscope (SEM) (Hitachi S-450). The fracture surface of an injection-moulded sample was obtained by quenching and breaking the sample in liquid nitrogen. For better characterization some dispersed TLCP phases were separated from the matrix polymer by selective dissolution. Small pieces of extrudates of TLCP1/PES, TLCP2/PES, TLCP4/PES and TLCP5/PES were immersed in *N,N*-dimethylformamide for 12 h to dissolve PES completely. The TLCP phase was separated by centrifuging the solution and decanting of the supernatant liquid. The centrifuged TLCP phase was immersed in fresh solvent and separated twice more. Finally a drop of the dispersion that was left was placed directly on an SEM sample holder, the solvent was evaporated off and the residue was coated with gold for observation. The diameter and intrinsic aspect ratio of TLCP droplets and fibrils were measured with a Cambridge Instrument Quantimet 520 Image Analysis System.

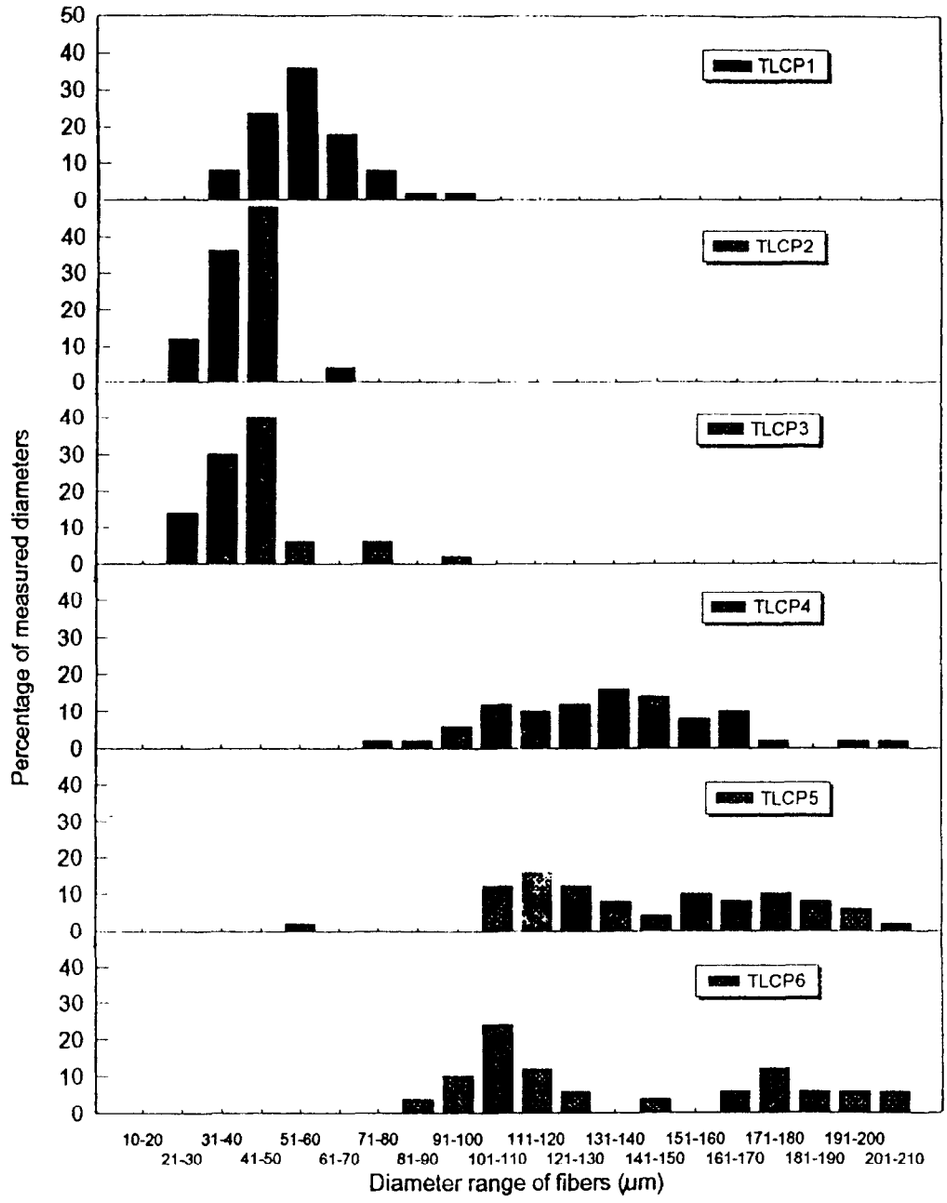

Figure 1 Diameter distribution of TLCP fibres: (a) TLCP1, (b) TLCP2, (c) TLCP3, (d) TLCP4, (e) TLCP5, (f) TLCP6

RESULTS AND DISCUSSION

Melt spinnability of TLCPs

At the optimized spinning temperature, shown in *Table 1*, six TLCPs were melt spun. The average diameter of TLCP fibres is shown in *Table 1* and the diameter distribution in *Figure 1*, respectively. According to the results, these six TLCPs can be divided into two groups. The first group consists of TLCP1, TLCP2 and TLCP3, characterized by small diameters and a narrow diameter distribution. The second group consists of TLCP4, TLCP5 and TLCP6, with larger diameters and a broader diameter distribution. Under the optimized spinning conditions, good spinnability is associated with small diameters and narrow diameter distribution of fibres. It is clear that the first group has better spinnability than the second group.

Wide-angle X-ray diffraction patterns of TLCP fibres show different degrees of orientation in these fibres, except the TLCP6. The degree of orientation of these fibres is consistent with their spinnability evaluated with their diameter and diameter distribution.

Effect of viscosity ratio on fibrillation

The fibrillation of TLCP in resin melt is influenced by a series of factors such as the composition of the blend, the viscosity of component polymers and their viscosity ratio, the processing temperature, the interfacial tension of polymer pairs and the shear rate. Among these the viscosity ratio of the dispersed TLCP to the matrix is a decisive factor[7,13,23]. A viscosity ratio far below unity favours the fibrillation of TLCP. However, the connection between the viscosity ratio and the spinnability has not yet been investigated. In this work, with the same TLCP, its morphology in different resins was observed and correlated with the viscosity ratio in a range of 10^{-2} to 10. The viscosity ratio, η_d/η_m, decreases from TLCP1/

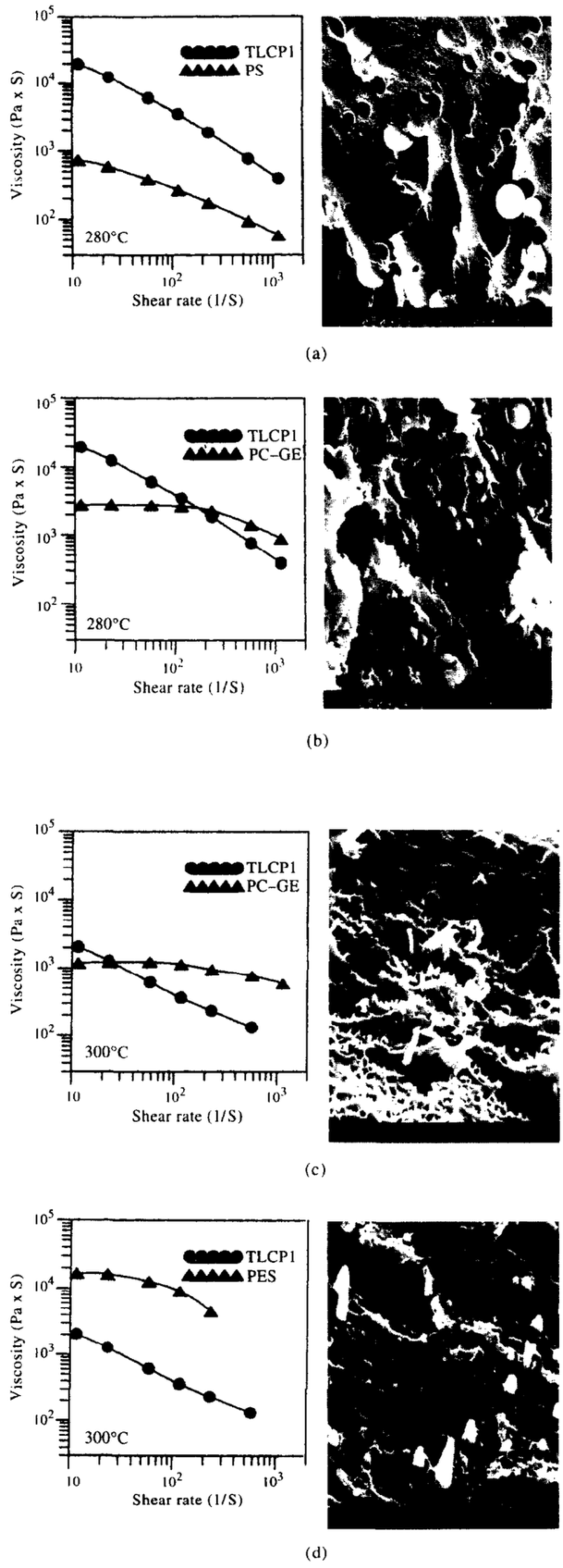

Figure 2 Rheological curves of component polymers and SEM micrographs of injection-moulded samples of their blends: (a) TLCP1 and PS at 280°C; (b) TLCP1 and PC-GE at 280°C; (c) TLCP1 and PC-GE at 300°C; (d) TLCP1 and PES at 300°C

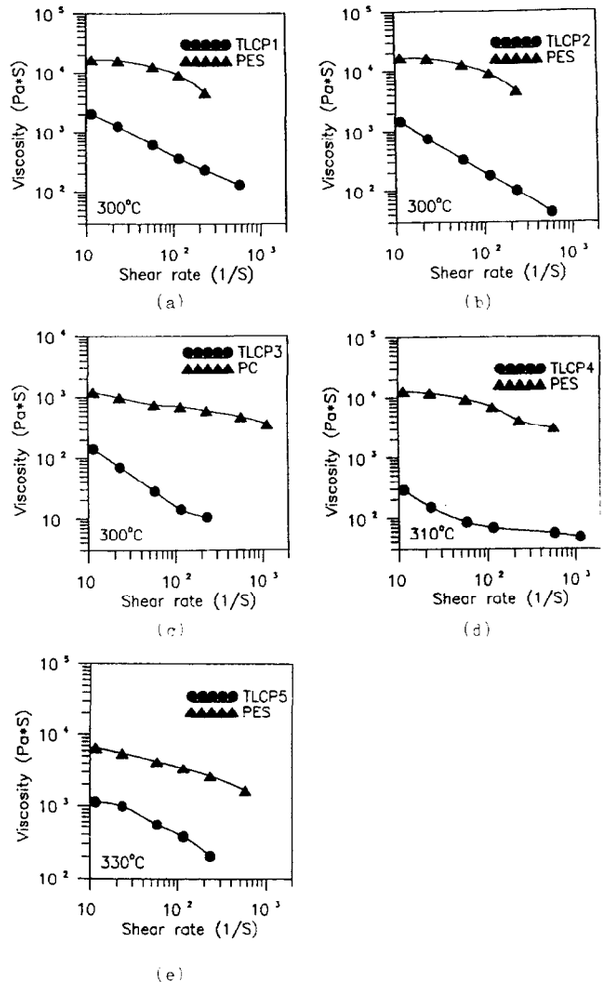

Figure 3 Rheological curves of TLCPs and matrices in viscosity ratio of 0.01 to 0.1: (a) TLCP1 and PES at 300°C; (b) TLCP2 and PES at 300°C; (c) TLCP3 and PC at 300°C; (d) TLCP4 and PES at 310°C; (e) TLCP5 and PES at 330°C

PS at 280°C, TLCP1/PC-GE at 280°C, TLCP1/PC-GE at 300°C to TLCP1/PES at 300°C. Viscosity curves of pure TLCP1 and matrix resins are shown in *Figure 2*, together with SEM micrographs of fracture surfaces of their injection-moulded samples for comparison. In *Figure 2a*, with the viscosity of TLCP1 10 times that of PS, TLCP1 spheres with diameters of 2–8 μm dispersed in PS matrix. In *Figure 2b* viscosity curves of TLCP1 and PC-GE at 280°C have a cross-over point. TLCP1 droplets have deformed spherical and ellipsoidal shapes with diameters of 1–3 μm. For TLCP1/PC-GE at 300°C (*Figure 2c*), the viscosity ratio is about 0.1. TLCP1 fibrils with diameters of 0.2–0.8 μm dispersed in PC-GE matrix. When the viscosity ratio is close to 0.01 (*Figure 2d*), TLCP1 droplets have large deformation; all of them have been elongated into fibrils with diameters of 0.05–0.1 μm. The results clearly show that with decreasing η_d/η_m the dispersed TLCP phase changes from spheres through ellipsoids to fibrils and the diameters of TLCP spheres or fibrils decrease. A low η_d/η_m favours the fibrillation of TLCP in molten resins, even for TLCPs having good spinnability, and a low viscosity ratio far below unity is necessary for the fibrillation. Submicrometre TLCP fibrils can be generated under certain conditions with TLCPs having good spinnability.

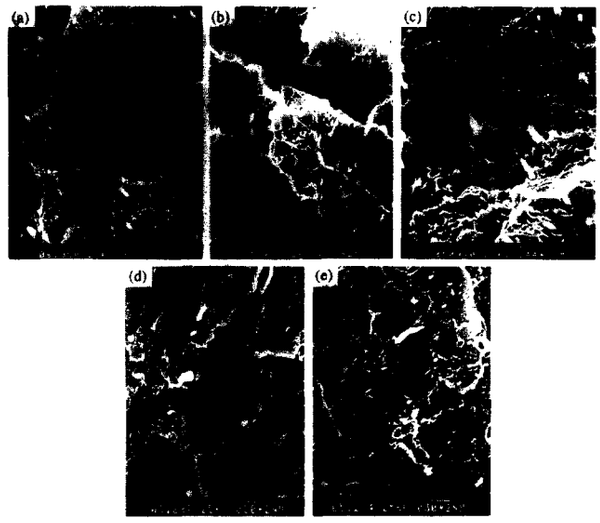

Figure 4 SEM photographs of fracture surface of injection-moulded samples: (a) TLCP1/PES at 300°C; (b) TLCP2/PES at 300°C; (c) TLCP3/PC at 300°C; (d) TLCP4/PES at 310°C; (e) TLCP5/PES at 330°C

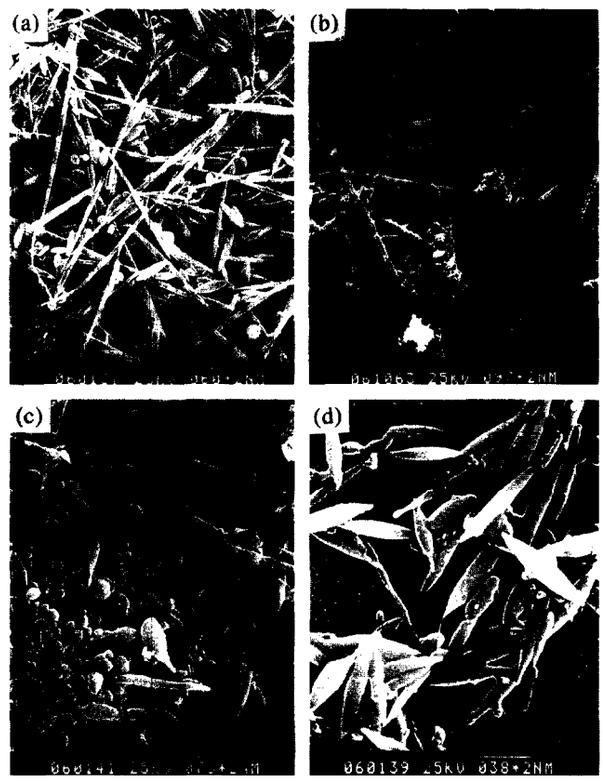

Figure 5 SEM micrographs of the dispersed TLCP phase extracted from extrudates of (a) TLCP1/PES (300°C), (b) TLCP2/PES (300°C), (c) TLCP4/PES (310°C), (d) TLCP5/PES (330°C)

Correlation between spinnability and fibrillation

For the investigation of the correlation between spinnability and fibrillation, the morphology of the dispersed TLCPs with different spinnabilities has been observed. In order to minimize the influence of the viscosity ratio, the study was conducted in a viscosity ratio range of 0.01 to 0.1, together with the same processing parameters.

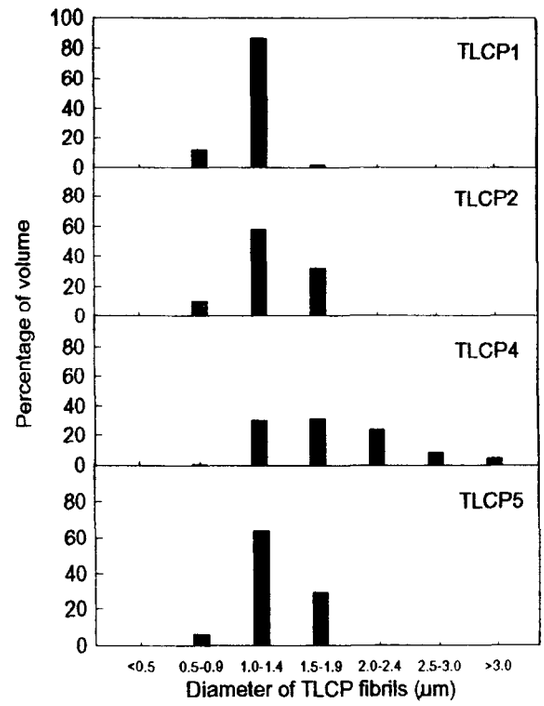

Figure 6 The diameter distribution of TLCP fibrils extracted from extrudates of (a) TLCP1/PES (300°C), (b) TLCP2/PES (300°C), (c) TLCP4/PES (310°C), (d) TLCP5/PES (330°C)

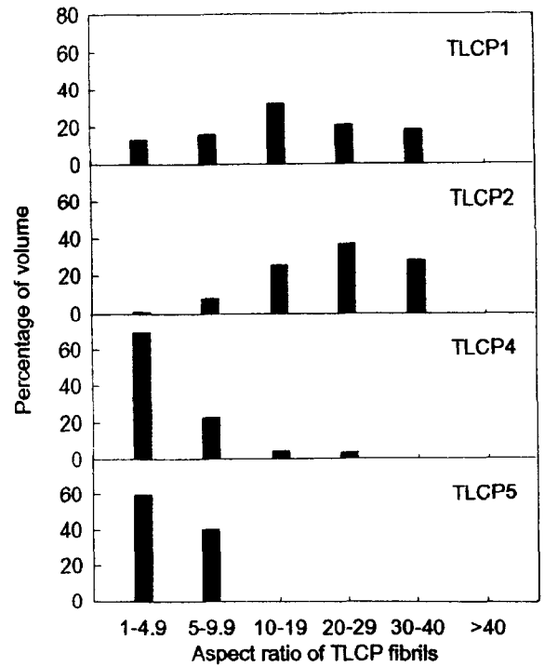

Figure 7 The aspect-ratio distribution of TLCP fibrils extracted from extrudates of (a) TLCP1/PES (300°C), (b) TLCP2/PES (300°C), (c) TLCP4/PES (310°C), (d) TLCP5/PES (330°C)

Figure 3 shows rheological curves of TLCP1/PES at 300°C, TLCP2/PES at 300°C, TLCP3/PC at 300°C, TLCP4/PES at 310°C and TLCP5/PES at 330°C. The fracture morphology of injection-moulded samples is shown in *Figure 4*. For TLCP1 and TLCP2 having good spinnability (*Figures 4a* and *4b*), the dispersed phase has

large deformation and droplets have been elongated into fibrils with diameters of 0.2–0.5 μm. In *Figure 4c*, TLCP3 phase has been deformed into rod-like fibre with diameters of 0.5–1 μm. However, for TLCP4 and TLCP5 having poor spinnability, spheres and elongated spheres with diameters of 0.3–2 μm are dispersed in the matrix (*Figures 4d* and *4e*).

In order to measure the diameter and aspect ratio of spheres and fibrils, the PES matrix in extrudates of TLCP1/PES, TLCP2/PES, TLCP4/PES and TLCP5/PES was dissolved by N,N-dimethylformamide. *Figure 5* shows the morphology of the dispersed TLCP phase in these blends. TLCP1 and TLCP2 have the form of fibrils mainly and short rods and ellipsoids, while TLCP4 and TLCP5 have the form of short rods and spheres. *Figures 6* and *7* show the diameter distribution and the aspect-ratio distribution of TLCP spheres and fibrils extracted from these four blends. It is clear that, compared to TLCP4 and TLCP5 having poor spinnability, the average diameter is smaller, the diameter distribution is narrower and the aspect ratio reaches higher values such as 40 for TLCP1 and TLCP2 having good spinnability.

All the results indicate that, under the same processing conditions, the good spinnability of TLCPs favours the fibrillation of TLCPs in resin melts. The latter is crucial to the submicrometre reinforcing function of TLCP for thermoplastics.

CONCLUSIONS

Based on the small diameter and the narrow diameter distribution of fibres spun from TLCPs at their respective optimized spinning temperatures, TLCP1, TLCP2 and TLCP3 have good spinnability. Low viscosity ratios far below unity are necessary for the fibrillation of TLCPs in resin melts, even for TLCPs having good spinnability. Under the same fibrillation conditions, including low viscosity ratios from 0.01 to 0.1, TLCPs having good spinnability generate fibrils with small diameters, narrow diameter distribution and large aspect ratios. All the results show a correlation between the spinnability of TLCPs in air and the fibrillation of TLCPs in resin melts. The spinnability of TLCPs can be taken as a prerequisite for the accomplishment of submicrometre reinforcing with TLCP fibrils.

ACKNOWLEDGEMENT

The authors are much indebted to Professor L. Nicolais for kindly supplying one of the TLCPs, Rhodester.

REFERENCES

1 Pawlikowski, G. T., Dutta, D. and Weiss, R. A. *Annu. Rev. Mater. Sci.* 1991, **21**, 159
2 Kiss, G. *Polym. Eng. Sci.* 1987, **27**, 410
3 Isayev, A. I. and Modic, M. *Polym. Compos.* 1987, **8**, 158
4 Dutta, D., Fruitwala, H., Kohli, A. and Weiss, R. A. *Polym. Eng. Sci.* 1990, **30**, 1005
5 Bretas, R. E. S. and Baird, D. G. *Polymer* 1992, **33**, 5233
6 Siegmann, A., Dagan, A. and Kenig, S. *Polymer* 1985, **26**, 1325
7 Blizard, K. G. and Baird, D. G. *Polym. Eng. Sci.* 1987, **27**, 653
8 Sharam, S. K., Tendolkar, A. and Misra, A. *Mol. Cryst. Liq. Cryst.* 1988, **157**, 597
9 Apicella, A., Iannelli, P., Nicodemo, L., Nicolais, L., Roviello, A. and Sirigu, A. *Polym. Eng. Sci.* 1986, **26**, 600
10 Zhuang, P., Kyu, T. and White, J. L. *Polym. Eng. Sci.* 1988, **28**, 1095
11 He, J., Zhang, H., Yuan, Q. and Xie, P. *Prog. Natural Sci.–Commun. State Key Lab. China* 1993, **3**, 214
12 He, J. and Bu, W. *Polymer* 1994, **35**, 5061
13 He, J., Bu, W. and Zhang, H. *Polym. Eng. Sci.* 1995, **35**, 1695
14 Taylor, G. I. *Proc. R. Soc. (A)* 1934, **146**, 501
15 Taylor, G. I. *Proc. R. Soc. (A)* 1932, **138**, 41
16 Van Oene, H. *J. Colloid Interface Sci.* 1972, **40**, 448
17 Chin, H. B. and Han, C. D. *J. Rheol* 1979, **23**, 557
18 Chin, H. B. and Han, C. D. *J. Rheol* 1980, **24**, 1
19 Tomotika, S. *Proc. R. Soc. (A)* 1935, **150**, 322
20 Pakula, T., Grebowicz, J. and Kryzewski, M. *Polym. Bull.* 1980, **2**, 799
21 He, J., Bu, W., Zhang, H., Xie, P. and Xu, X. *Int. Polym. Process.* 1993, **8**, 129
22 Suto, S., White, J. L. and Fellers, J. F. *Rheol. Acta* 1982, **21**, 62
23 Beery, D., Kenig, S. and Siegmann, A. *Polym. Eng. Sci.* 1991, **31**, 451